

Lawrence Berkeley National Laboratory

Lawrence Berkeley National Laboratory

Title

The effect of thin film thickness on the incorporation of Mn interstitials in Ga_{1-x}Mn_xAs

Permalink

<https://escholarship.org/uc/item/0k57z6n1>

Authors

Yu, K.M.
Walukiewicz, W.
Wojtowicz, T.
[et al.](#)

Publication Date

2004-10-05

Peer reviewed

The Effect of Film Thickness on the Incorporation of Mn Interstitials in $\text{Ga}_{1-x}\text{Mn}_x\text{As}$

K. M. Yu¹, W. Walukiewicz¹, T. Wojtowicz^{2,3}, J. Denlinger⁴, M. A. Scarpulla⁵, X. Liu³,
and J. K. Furdyna³

¹Electronic Materials Program, Materials Sciences Division,
Lawrence Berkeley National Laboratory, Berkeley, CA 94720

²Institute of Physics, Polish Academy of Sciences, 02-668 Warsaw, Poland

³Department of Physics, University of Notre Dame, Notre Dame, IN 46556

⁴Advanced Light Source, Lawrence Berkeley National Laboratory, Berkeley, CA 94720

⁵Department of Materials Sciences and Mineral Engineering, University of California,
Berkeley, California 94720

ABSTRACT

We have investigated the effect of film thickness on the distribution of Mn atoms at various lattice sites in $\text{Ga}_{1-x}\text{Mn}_x\text{As}$ thin films. We find that the growth surface acts as a sink facilitating the out-diffusion of Mn interstitials (Mn_I), and thus reducing its concentration in the film. The out-diffused Mn_I accumulate on the surface in a surface oxide layer and do not participate in the ferromagnetism of the film. For thin films less than 15 nm thick, no Mn_I can be detected. Because of the absence of compensating Mn_I defects, higher T_C can be achieved for such extremely thin $\text{Ga}_{1-x}\text{Mn}_x\text{As}$ layers. These results agree with our previously suggested Fermi-level-governed upper limit of the T_C of III-Mn-V ferromagnetic semiconductors.

PACS numbers: 75.50.Pp, 72.80.Ey, 73.61.Ey, 75.70.-I

It is generally accepted that Mn atoms in substitutional Ga site (Mn_{Ga}) provide free holes that mediate the ferromagnetic interaction between the Mn magnetic moments in ferromagnetic $\text{Ga}_{1-x}\text{Mn}_x\text{As}$ alloys [1-3]. Using ion channeling methods, we have shown that in addition to substituting for Ga, a fraction of Mn atoms reside in interstitial sites (Mn_{I}) in $\text{Ga}_{1-x}\text{Mn}_x\text{As}$ [4]. The Mn_{I} are double donors that compensate Mn_{Ga} acceptors, thus leading to a saturation of the free hole concentration. They also tend to align antiferromagnetically with the spins of Mn_{Ga} , thus reducing the total net magnetic moment due to Mn. Finally, the spins of isolated Mn_{I} do not contribute to ferromagnetism because of their negligible p - d exchange hybridization [5]. These three effects limit the maximum Curie temperature T_{C} in the “bulk-like” $\text{Ga}_{1-x}\text{Mn}_x\text{As}$ to approximately 110 K. The incorporation of Mn_{I} in GaAs was subsequently calculated to be energetically favorable under non-equilibrium growth conditions [6-8]. Our recent studies on Be doped $\text{Ga}_{1-x}\text{Mn}_x\text{As}$ [9] and modulation doped $\text{Ga}_{1-y}\text{Al}_y\text{As}/\text{Ga}_{1-x}\text{Mn}_x\text{As}/\text{Ga}_{1-y}\text{Al}_y\text{As}$ heterostructures (MDHs) [10,11] have further confirmed that the formation of Mn_{I} and the saturation of the T_{C} is controlled by the position of the Fermi energy.

Recently, T_{C} 's exceeding the 110 K limit have been reported in thin $\text{Ga}_{1-x}\text{Mn}_x\text{As}$ films (<50 nm thick) after low temperature annealing [12,13]. Ku *et al.* noted that, while they achieved a maximum T_{C} of 150 K for 20 nm $\text{Ga}_{1-x}\text{Mn}_x\text{As}$ films, they did not succeed in achieving $T_{\text{C}} > 110\text{K}$ for samples thicker than 50 nm [13]. These findings suggest that for very thin layers surface and/or interfacial effects may play a role in increasing T_{C} to values beyond the limitation set forth by the Fermi level. In this paper, we address the issue of film thickness on ferromagnetism of $\text{Ga}_{1-x}\text{Mn}_x\text{As}$ by investigating the lattice location of Mn atoms in the GaAs lattice as a function of film thickness.

A series of $\text{Ga}_{1-x}\text{Mn}_x\text{As}$ films with thicknesses ranging from 14 to 200 nm and Mn concentration in the range from 7 to 10% were grown on semi-insulating (001) GaAs substrates in a Riber 32 R&D molecular beam epitaxy system at a growth temperature of 210°C [4,6]. Magnetoresistance, Hall Effect, and superconducting quantum interference device (SQUID) magnetometry were used for electrical and magnetic characterization and for determining T_C . The lattice locations of Mn sites in the $\text{Ga}_{1-x}\text{Mn}_x\text{As}$ lattice were studied by combined channeling particle-induced x-ray emission (c-PIXE) and Rutherford backscattering (c-RBS) [4,9].

Figure 1 shows the normalized yields χ of the Mn (PIXE) and GaAs (RBS) signals from 14 nm and 100 nm $\text{Ga}_{1-x}\text{Mn}_x\text{As}$ films as functions of the incident beam angles about the $\langle 110 \rangle$ and $\langle 111 \rangle$ axes (angular scans). Here χ is the ratio of the channeled yield to the corresponding unaligned yield. We note that atoms in interstitial positions (tetrahedral or hexagonal) in the zinc-blende lattice are shadowed by the host atoms when viewed along the $\langle 100 \rangle$ and $\langle 111 \rangle$ axial channels, but are exposed in the $\langle 110 \rangle$ axial channel [14]. For the 14 nm thick sample (upper panels) both the Mn and host GaAs scans in the $\langle 110 \rangle$ and $\langle 111 \rangle$ directions are very similar, with the χ_{Mn} much higher than the host χ_{GaAs} . This indicates that the Mn atoms are incorporated in this 14 nm thick $\text{Ga}_{1-x}\text{Mn}_x\text{As}$ layer ($x=0.1$) either in substitutional Ga sites (Mn_{Ga} fraction $\sim 70\%$) or in random positions (Mn_{rand} fraction $\sim 30\%$) non-commensurate with the lattice. The fraction of Mn_i in this sample is below the detection limit of the channeling technique ($< 2\%$ of the total Mn).

The channeling results for the 14 nm $\text{Ga}_{1-x}\text{Mn}_x\text{As}$ layer are in striking contrast to the results we reported for $\text{Ga}_{1-x}\text{Mn}_x\text{As}$ films thicker than 50 nm where we found

substantial fraction of Mn in interstitial positions [4]. As an example, we show the angular scans for a 100 nm thick $\text{Ga}_{1-x}\text{Mn}_x\text{As}$ layer ($x=0.09$) in the lower panels of Fig. 1. In this thick sample, χ_{Mn} is only slightly higher than χ_{GaAs} for the $\langle 111 \rangle$ channeling direction, suggesting that a small fraction of Mn is in random positions (random fraction $\sim 5\%$). The much higher values of χ_{Mn} in the $\langle 110 \rangle$ scans can be interpreted as due to the presence of *interstitial* Mn atoms. The fraction of Mn_I in this sample can be estimated be $\sim 14\%$ [4,14]. We note that SQUID magnetometry measurement shows T_C of 110K and 65K for the thin and thick $\text{Ga}_{1-x}\text{Mn}_x\text{As}$ samples shown in Fig. 1, respectively. We attribute the lower T_C in the thick sample to the presence of Mn_I which electrically compensate the Mn_{Ga} acceptors and cancel the Mn_{Ga} spins [4, 9].

In a recent report, Edmonds *et al.* [15] found that Mn_I are relatively mobile and have a tendency to out-diffuse to the surface during post-growth low temperature annealing. Such Mn_I out-diffusion was found to be governed by an energy barrier of ~ 0.7 eV. As a result of the Mn_I diffusion, a Mn-rich oxide layer was detected on the surface of $\text{Ga}_{1-x}\text{Mn}_x\text{As}$ that can be etched off by HCl [16]. We believe that the large fraction of Mn_{rand} ($\sim 30\%$) which we observe in the 14 nm $\text{Ga}_{1-x}\text{Mn}_x\text{As}$ film comes from the Mn in the surface oxide layer due to the out-diffusion of Mn_I . Because of the small thickness of the film, it is possible that this out-diffusion process occurred during growth and the Mn-rich layer subsequently oxidized when the film was exposed to air.

Channeling RBS and PIXE measurements on the 14 nm layer after etching in HCl show that the removal of the ~ 2 nm thick surface layer leads to a $\sim 25\%$ reduction in the total Mn concentration and a reduction of Mn_{rand} from ~ 30 to 15% . This suggests that the oxide surface layer is Mn-rich and contains $\sim 8 \times 10^{14}/\text{cm}^2$ of Mn_{rand} . The $\sim 15\%$ Mn_{rand}

still present in the etched sample most probably exists in the form of small Mn-related clusters. Furthermore, magnetization measurements before and after the HCl etching shows essentially identical results for both T_C and for saturation magnetization, suggesting that the Mn_{rand} in the oxide layer do not participate in the carrier-mediated ferromagnetism.

This interpretation of the RBS/PIXE results is confirmed by the x-ray absorption spectroscopy (XAS) measurements obtained in total electron yield mode at room temperature at beamline 8.0 of the Advanced Light Source. Figure 2 shows the Mn 2p \rightarrow 3d XAS spectra for the 14 nm thick sample before and after the HCl etching. As other researchers have demonstrated previously, the XAS spectrum for the as-grown sample shows a main peak for the L_3 level at 640 eV, with a shoulder at ~ 0.5 eV lower in energy [16,17]. Ishiwata *et al.* [17] interpreted this low-energy shoulder as being due to metastable paramagnetic defects due to coupling with excess As. They argued that these defects transformed into the ferromagnetic component that gave rise to the higher energy peak with low temperature annealing. Figure 2 shows that only the low-energy peak remains after the removal of the Mn-rich oxide layer by HCl etching. XAS measurements on ZnMnOTe alloys also indicate that the absorption peak at 640 eV indeed comes from Mn-O bonds. This strongly suggests that the high-energy “major” peak in the XAS spectrum from the as-grown layer is due to Mn in the oxide layer, while the lower energy peak in the doublet arises from Mn_{Ga} . This is in agreement with the recent report by Edmonds *et al.*, who identified a Mn-rich oxide layer and further correlated this low-energy peak with large X-ray magnetic circular dichroism [17].

Figure 3 shows the distribution of Mn in various lattice sites in $\text{Ga}_{1-x}\text{Mn}_x\text{As}$ films ($x \sim 0.07-0.10$) with thicknesses ranging from 14 to 120 nm obtained by ion channeling. A monotonic increase in the Mn_I fraction and a corresponding decrease in the Mn_rand fraction are observed with increasing film thickness. Above a film thickness of 60 nm the relative amounts of Mn_I and Mn_rand remain rather constant. To understand the origin of this limiting film thickness, we note that for the thin samples the areal density of Mn atoms in the surface oxide layer is relatively independent of film thickness, and is approximately equal to $8 \times 10^{14} \text{ cm}^{-2}$. This is close to the density of Ga sites on the (001) surface, suggesting that the out-diffusion of the Mn_I during the growth, or after it is exposed to air, is limited by the accumulation of approximately one monolayer of Mn on the surface. Note that for a Mn_I fraction of 15% in a 15 nm film with $x=0.10$, $[\text{Mn}_\text{I}] = 5 \times 10^{14} \text{ cm}^{-2}$. For films with thicknesses of ~ 10 nm, the diffusion length of Mn_I in the film is comparable to the film thickness [15], and it is therefore conceivable that this Mn_I out-diffusion can account for the elimination of Mn_I in very thin films. At higher film thicknesses Mn_I out-diffusion affects only the outer thin layer, and is limited by the accumulation of ~ 1 monolayer of Mn on the surface, while the remaining Mn_I are incorporated in the bulk of the layer. The electronic and magnetic properties of these thick films are then determined by a balance between Mn_Ga , Mn_I and Mn_rand .

The distribution of Mn in the 14 and 22 nm $\text{Ga}_{1-x}\text{Mn}_x\text{As}$ films after HCl etching are also shown in Fig. 3. An increase in the fraction of Mn_Ga is observed in both these thin samples due to the removal of the Mn-rich oxide layer. We also note that, except for the 14 nm thick film, the net concentrations of Mn_Ga in the $\text{Ga}_{1-x}\text{Mn}_x\text{As}$ films are in the range of $1.0-1.3 \times 10^{21} \text{ cm}^{-3}$. This is close to the maximum hole concentration of

$\sim 1 \times 10^{21} \text{ cm}^{-3}$ in $\text{Ga}_{1-x}\text{Mn}_x\text{As}$, that corresponds to the maximum Fermi energy E_{Fmax} we reported previously [4]. However, we estimate the concentration of Mn_{Ga} to be $\sim 1.7 \times 10^{21} \text{ cm}^{-3}$ for the 14 nm thick film. This enhancement in the incorporation of Mn_{Ga} could be partially explained by Fermi level pinning at the free surface and at the interface between the GaMnAs layer and the underlying LT-GaAs. Such pinning would raise the Fermi energy, thus giving rise -- by lowering the formation energy of Mn_{Ga} -- to the higher T_{C} observed in thin layers without post growth annealing

In summary we have investigated the effect of film thickness on the Mn lattice location in ferromagnetic $\text{Ga}_{1-x}\text{Mn}_x\text{As}$ thin films. We find that for film thicknesses less than 60 nm, the growth surface acts as a sink which facilitates the out-diffusion of Mn_{I} , thus reducing its concentration in the film. For the $\text{Ga}_{1-x}\text{Mn}_x\text{As}$ film thicknesses below 15 nm no Mn_{I} could be detected. One can thus conclude that, because of the absence of compensating Mn_{I} defects, higher T_{C} can be achieved for such extremely thin $\text{Ga}_{1-x}\text{Mn}_x\text{As}$ layers. Most of the Mn not incorporated as Mn_{Ga} in this case accumulate as a surface oxide layer, and do not participate in the ferromagnetism of the film. These results are fully consistent with our previously proposed model of Fermi-level-controlled upper limit of T_{C} in III-Mn-V ferromagnetic semiconductors.

This work was supported by the Director, Office of Science, Office of Basic Energy Sciences, Division of Materials Sciences and Engineering, of the U. S. Department of Energy under Contract No. DE-AC03-76SF00098; by National Science Foundation Grant DMR02-10519; and by the DARPA SpinS Program.

REFERENCES

1. H. Ohno, *Science* **281**, 951 (1998).
2. T. Dietl, *Semicond. Sci. Technol.* **17**, 377 (2002).
3. T. Dietl, H. Ohno, F. Matsukura, J. Cibert, and D. Ferrand, *Science* **287**, 1019 (2000).
4. K. M. Yu, W. Walukiewicz, T. Wojtowicz, I. Kuryliszyn, X. Liu, Y. Sasaki, and J. K. Furdyna, *Phys. Rev. B* **65**, 201303-1(R) (2002).
5. J. Blinowski and P. Kacman, *Phys. Rev. B* **67**, 121204(R) (2003).
6. F. Maca and J. Masek, *Phys. Rev. B* **65**, 235209 (2002).
7. S. C. Erwin and A. G. Petukov, *Phys. Rev. Lett.* **89**, 227201 (2002).
8. Priya Mahadevan and Alex Zunger, *Phys. Rev. B* **68**, 075202 (2003).
9. K. M. Yu, W. Walukiewicz, T. Wojtowicz, W. L. Lim, X. Liu, Y. Sasaki, M. Dobrowolska, and J. K. Furdyna, *Phys. Rev. B* **68**, 041308-1(R) (2003).
10. T. Wojtowicz, W.L. Lim, X. Liu, M. Dobrowolska, J. K. Furdyna, K. M. Yu, W. Walukiewicz, I. Vurgaftman, and J. R. Meyer, *Appl. Phys. Lett.* **83**, 4220 (2003).
11. K. M. Yu, W. Walukiewicz, T. Wojtowicz, W.L. Lim, X. Liu, M. Dobrowolska, and J. K. Furdyna, *Appl. Phys. Lett.* **84**, 8325 (2004)
12. D. Chiba, K. Takamura, F. Matsukura, and H. Ohno, *Appl. Phys. Lett.* **82**, 3020 (2003).
13. K. C. Ku, S. J. Potashnik, R. F. Wang, S. H. Chun, P. Schiffer, N. Samarth, M. J. Seong, A. Mascarenhas, E. Johnston-Halperin, R. C. Myers, A. C. Gossard, and D. D. Awschalom, *Appl. Phys. Lett.* **82**, 2302 (2003).

14. L. Feldman, J. W. Mayer, and S. T. Picraux, *Materials Analysis by Ion Channeling* (Academic, New York, 1982).
15. K.W. Edmonds, P. Boguslawski, B.L. Gallagher, R.P. Champion, K.Y. Wang, N.R.S. Farley, C.T. Foxon, M. Sawicki, T. Dietl, M. Buongiorno Nardelli, J. Bernholc, Phys. Rev. Lett. **92**, 037201 (2004)
16. K. W. Edmonds, N. R. S. Farley, R. P. Champion, C. T. Foxon, and B. L. Gallagher T. K. Johal and G. van der Laan M. MacKenzie and J. N. Chapman E. Arenholz, Appl. Phys. Lett. **84**, 4065 (2004).
17. Y. Ishiwata, M. Watanabe, R. Eguchi, T. Takeuchi, Y. Harada, A. Chainani, S. Shin, T. Hayashi, Y. Hashimoto, S. Katsumoto, and Y. Iye, Phys. Rev. **B65**, 233201 (2002).

FIGURE CAPTIONS

Fig. 1 Angular scans of the Mn K x-rays and GaAs RBS signals observed about the $\langle 110 \rangle$ and $\langle 111 \rangle$ axes for two $\text{Ga}_{1-x}\text{Mn}_x\text{As}$ samples: a 14 nm thick film with $x=0.10$ (upper panels); and a 100 nm thick film with $x=0.09$ (lower panels).

Fig. 2 Mn $2p$ XAS spectra for a 14 nm thick $\text{Ga}_{1-x}\text{Mn}_x\text{As}$ sample, as-grown and after HCl etching.

Fig. 3 The fractions of Mn occupying various lattice sites -- substitutional (Mn_{Ga}), interstitial (Mn_{I}) and in random-cluster form (Mn_{rand}) -- measured by channeling techniques for $\text{Ga}_{1-x}\text{Mn}_x\text{As}$ samples with film thicknesses between 14 and 120 nm. Data for 14 and 21.7 nm $\text{Ga}_{1-x}\text{Mn}_x\text{As}$ films etched by HCl are also shown as open symbols.

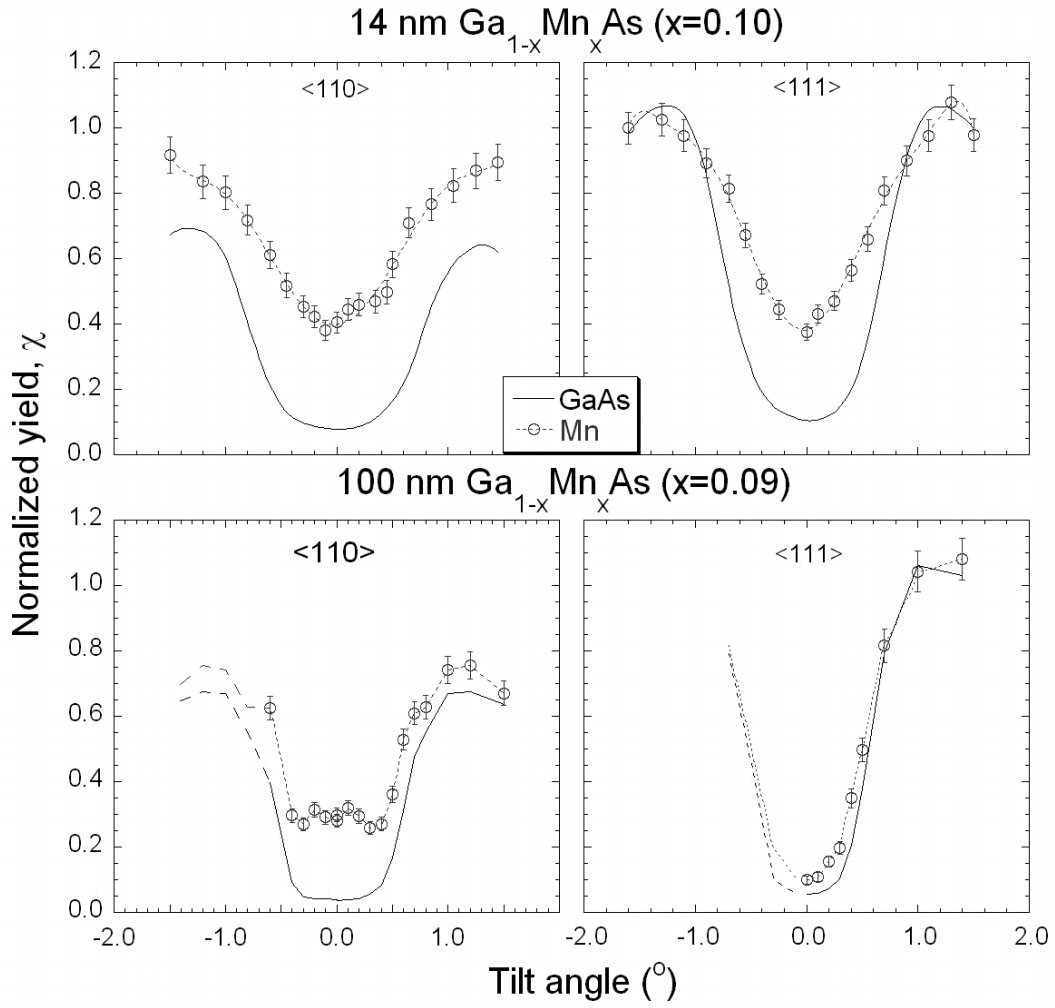


Fig. 1

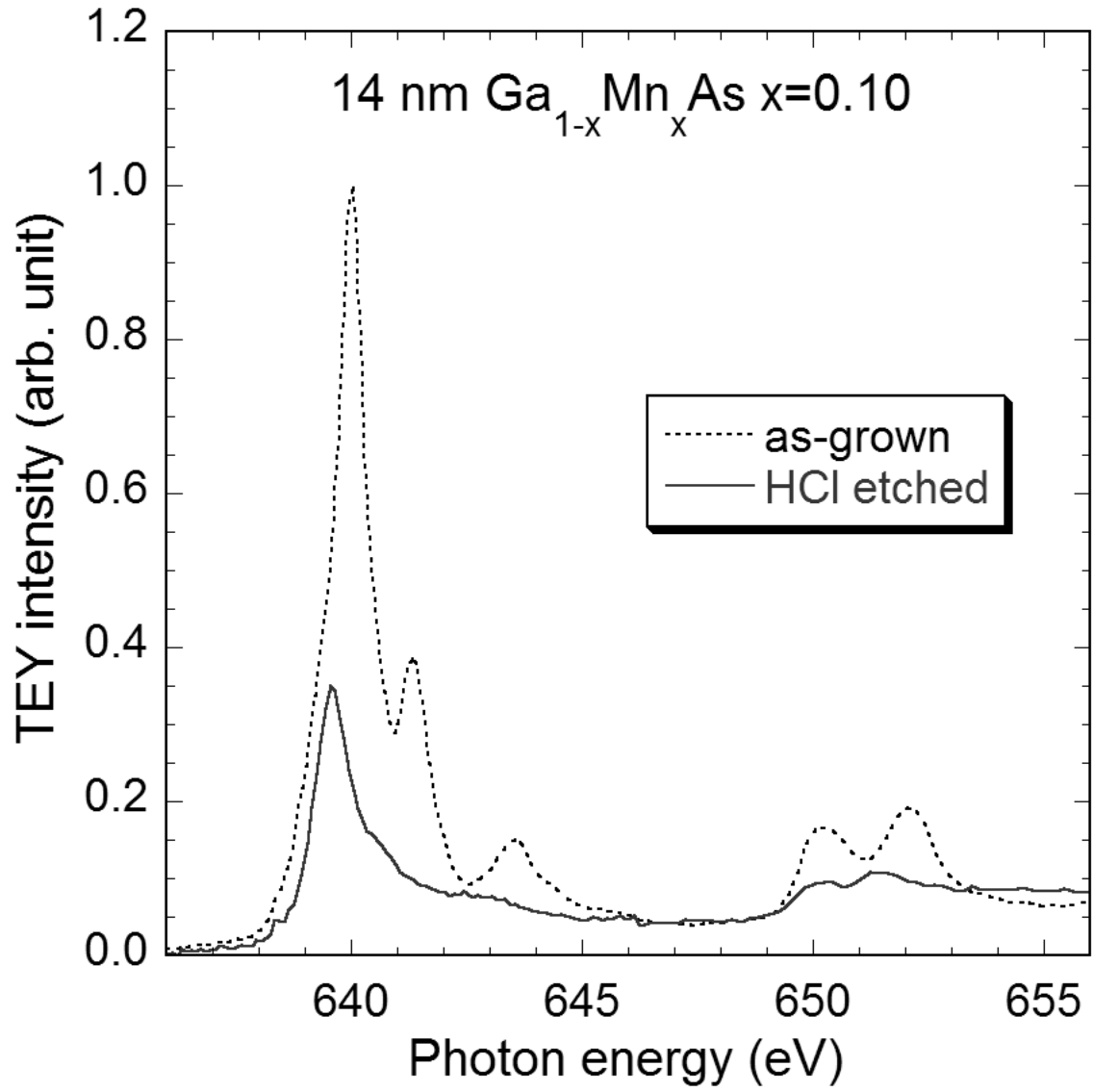


Fig. 2

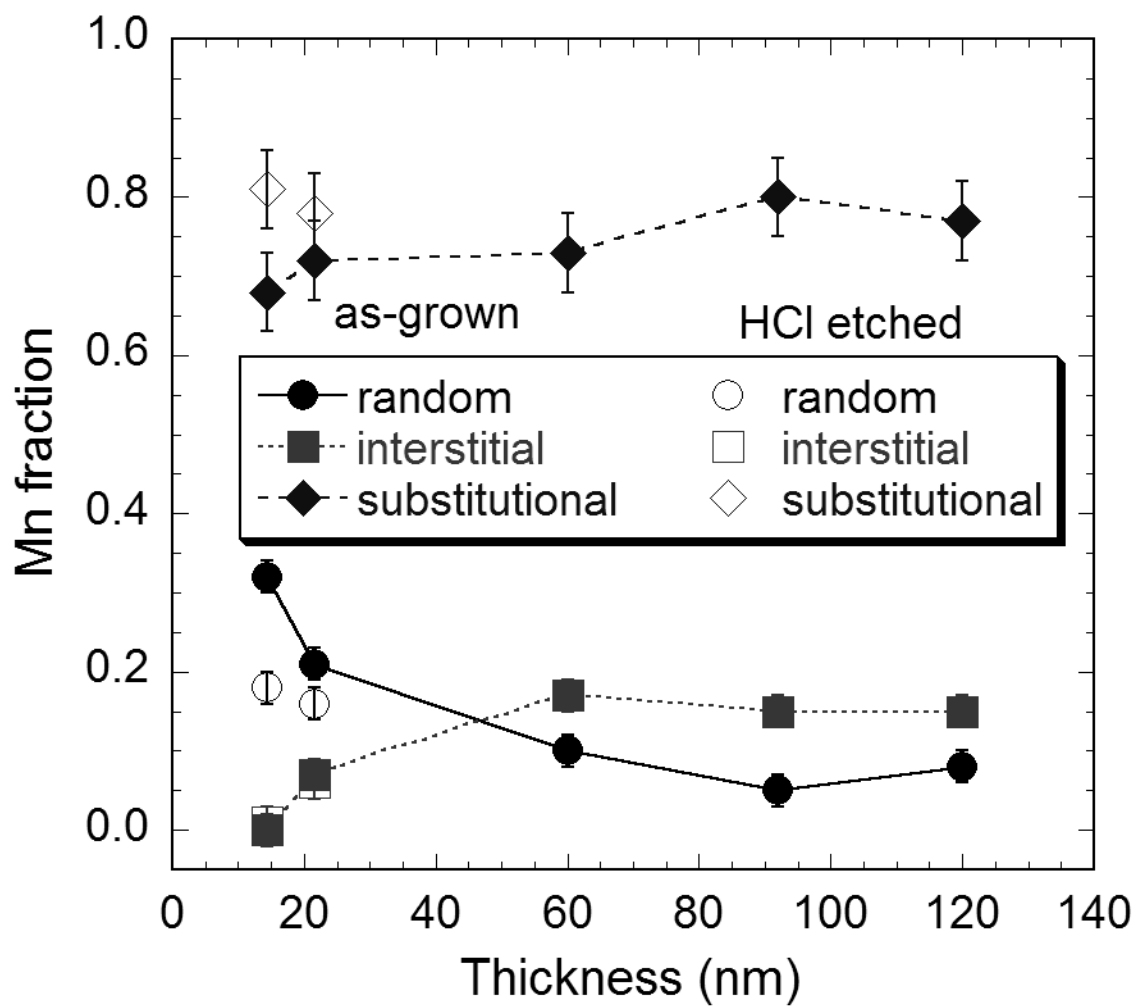


Fig. 3